Journal of Applied Polymer Science

Mesomorphic Phase Formation of Plasticized Poly(L-lactic acid)

Shunsuke Koido,[1] Takahiko Kawai,[1] Shinichi Kuroda,[1] Koji Nishida,[2] Toshiji Kanaya,[2] Makoto Kato,[3] Takashi Kurose,[4] Katsuhiko Nakajima[4]

[1]Graduate School of Engineering, Gunma University, Ota, Gunma 373-0057, Japan
[2]Institute for Chemical Research, Kyoto University, Uji, Kyoto 611-0011, Japan
[3]Toyota Central R&D Labs Inc., Nagakute, Aichi 480-1192, Japan
[4]Toyota Motor Corporation, Toyota, Aichi 410-1193, Japan
Correspondence to: T. Kawai (E-mail: kawaitakahiko@gunma-u.ac.jp)

ABSTRACT: The effects of the crystallization temperature, T_c, on the crystal structure as well as its thermal behavior of plasticized poly(L-lactic acid) were investigated by means of wide-angle X-ray diffraction (WAXD), Fourier-transform infrared spectroscopy (FTIR), and differential scanning calorimetry (DSC). PLLA blended with succinic acid-bis[2-[2-(2-methoxyethoxy)ethoxy]ethyl] ester (SAE) showed clear difference in T_c dependence of crystalline form compared to PLLA homopolymer. PLLA with 26 wt % SAE crystallized into orthorhombic α form for T_c above 80°C, while a peculiar disordered structure (mesophase) was obtained for T_c at 40°C. A detailed FTIR analysis of the mesophase of PLLA, focusing on the intra- and inter-chain interaction in the structure, indicated that mesophase had a large degree of disorder in 10/3 helical conformation as well as its packing manner of disordered 10/3 helical chain. Upon heating, mesophase showed a steep exothermic peak at 80°C in DSC thermogram, indicating the phase transformation from mesophase to a form crystal. FTIR results showed that the degree of interchain interaction of C=O in PLLA started to decrease above 60°C, followed by steep increase at 80°C due to the recrystallization into a form. Melt-recrystallization process in mesophase-α transformation was clarified. © 2013 Wiley Periodicals, Inc. J. Appl. Polym. Sci. **2014**, *131*, 39762.

KEYWORDS: plasticizer; crystallization; lattices; biopolymers and renewable polymers; phase behavior

Received 2 April 2013; accepted 15 July 2013
DOI: 10.1002/app.39762

INTRODUCTION

Poly(L-lactic acid) (PLLA) is a type of biodegradable polymer, which can also be produced from renewable resources. PLLA is attracting much attention from the ecological point of view and the expansion of industrial application of PLLA is being expected. One of the most concerning issues in the crystallization of PLLA is its crystallization kinetics. It has been reported that the crystallization rate of PLLA is extraordinary slow compared to the other polymers, including isotactic polypropylene (iPP) that has almost the same melting point.[1,2] Many efforts have been made to accelerate the crystallization of PLLA in recent years.[3–5]

Among various methods for accelerating crystallization rate of polymers, the nucleating agents are widely used in industry. A nucleating agent is, in general, an organic or inorganic material, which remains unmelted in a polymer melt and supplies an active surface for the polymer to nucleate during cooling. Various nucleating agents were reported to have sufficient effects on PLLA crystallization although the mechanism is not fully understood.[3,4] In addition to the nucleating agent, we have reported that the addition of poly(D-lactic acid), known as the enantiomer of PLLA, also shows a great enhancement in the crystallization rate of PLLA.[5]

A plasticizer is known as a type of additive, which affects the fundamental properties of a polymer such as melt viscosity and glass transition temperature (T_g).[6–9] In addition to the controllability of the mechanical properties, a plasticizer also affects the crystallization kinetics of polymer since the mobility of polymer chain is greatly affected. In our previous work,[10] we have studied the effect of the addition of succinic acid-bis[2-[2-(2-methoxyethoxy)ethoxy]ethyl] ester (SAE) as a plasticizer on the crystallization behavior of PLLA by small-angle X-ray scattering (SAXS) and wide-angle X-ray diffraction (WAXD). A large accelerative effect in PLLA crystallization was investigated especially at lower crystallization temperature (T_c = 80°C). It implies that the addition of SAE reduces the chain entanglement of PLLA in the molten state, leading to the enhancement of the chain mobility during the crystallization process. Moreover, we have also reported that the crystalline form of PLLA varies both with the concentration of SAE. However, the effect of T_c on the crystalline form of plasticized PLLA remains unsolved.

Depending on the preparation conditions, three different crystalline forms (α, β, γ) can be obtained for PLLA.[11–13] Crystallization from the melt or from solution leads to α form, which is the most common crystalline form. In the α form, two chains with 10/3 helical conformation are packed into an orthorhombic unit cell with the dimensions of a = 10.7 Å, b = 6.45 Å, and c (fiber axis) = 27.8 Å. Recently, we have reported that another disordered-type crystal form, the α' form, is formed at lower T_c.[13] The α form and the α' form were obtained when the T_c was above 120°C and below 90°C, respectively. The α' form is considered to have a considerable amount of interchain disorder in the unit cell, which leads to the slight expansion (*ca.* 1%) in the lateral dimension of the unit cell. Since the crystalline form of semicrystalline polymer has a strong influence especially on the thermal behavior, the studies both on the crystalline structure and the thermal behavior of polymer is essentially important.

In this study, our aim is to understand the effect of T_c on the crystalline structure of plasticized PLLA. A detailed structure analysis by means of Fourier transform infrared spectra (FTIR) is to be shown in order to discuss the intra- and inter-chain interaction in the crystalline structure formed at various temperatures. The changes in the crystalline structure upon heating are also presented.

MATERIALS AND METHODS

PLLA with a molecular weight M_w of 100,000 g/mol used in this study. The ester compound called succinic acid-bis[2-[2-(2-methoxyethoxy)ethoxy]ethyl] ester (SAE) ($C_{18}H_{34}O_{10}$, M_w = 410 g/mol) was used as a plasticizer. These materials were supplied by Toyota Motor Corporation. The PLLA pellets were dried at 80°C for 12 h before use, followed by melt blended with 26 wt % of SAE with an aid of extruder at 200°C. The PLLA/SAE samples were then melted to erase previous thermal history, followed by quenching into ice water to obtain an amorphous film with the thickness of 500 μm for WAXD measurement and 50 μm for FTIR measurement. The glass transition temperatures of PLLA and PLLA/SAE (26 wt %), measured by differential scanning calorimetry (DSC) heating scan for the samples quenched at −100°C from the melt, were 59.4°C and 0.0°C, respectively.

WAXD

WAXD measurement was performed using the beam line BL-40B2 at SPring-8, Himeji, Japan. The wavelength of the incident X-ray beam and the camera distance were 0.1 nm and 57 mm, respectively. The PLLA/SAE samples for WAXD measurements were sandwiched between thin kapton films and melted at 200°C for 2 min, followed by annealing in oil bath which was kept at various temperatures for isothermal crystallization (40–120°C).

FTIR

FTIR spectra were measured with a JASCO FTIR-4200 spectrometer equipped with a TGS detector. The PLLA/SAE samples for IR measurement were sandwiched between KBr disks and melted at 200°C for 2 min, followed by annealing in temperature control cell for isothermal crystallization at various T_c (40–120°C). The spectra were obtained by coadding 128 scans at a 2 cm^{-1} resolution. For studying the thermal behavior of crystallized PLLA/SAE blend via *in situ* FTIR measurement, the sample was set in a temperature control cell placed in the sample compartment of the spectrometer. During heating process with a constant heating rate of 1°C/min, FTIR spectra of the specimens were recorded at 1°C intervals from 40 to 200°C with 1 min intervals. The spectra were obtained by coadding 32 scans at a 2 cm^{-1} resolution.

Differential Scanning Calorimetry

Thermal behavior of PLLA/SAE blends was analyzed by Perkin Elmer Pyris1 DSC, which was calibrated by the melting of indium and tin. A fixed heating rate of 10°C/min was applied for the samples precrystallized at various T_c (40–120°C) in a flowing-nitrogen atmosphere.

RESULTS AND DISCUSSION

Crystal Structure of PLLA/SAE Blends

Figure 1 shows the WAXD profiles of the sample, crystallized at various temperatures from the melt. For the T_c above 60°C, sharp diffractions can be seen, indicating that the crystals are formed. The diffractions in Figure 1 from lower q were assigned to (010), (110)/(200), (113)/(203), and (210) of α form of PLLA.[2,13,14]

Whereas for T_c at 40°C, very broad diffractions at q = 11.7 and 22.4 nm^{-1} are observed, which can be assigned to the interchain and the intrachain distance of 10/3 helix of PLLA chain, respectively. Comparing to the WAXD pattern of amorphous PLLA, the structure formed at 40°C differs from that of crystal and amorphous. Moreover the broad peak of (110) shows low-q shift compared to that of (110)/(200) of α form, indicating a longer interchain distance in the sample crystallized at 40°C. Above difference in WAXD pattern leads to the conclusion that the structure formed at 40°C is so called mesophase that has an intermediate order between amorphous and crystal structures.

The disordered-type structures have been observed in some homopolymers.[15–20] iPP is known to form mesophase by quenching into iced water from the melt. The mesophase is reported to have 3/1 helix as in the crystal (α form) and a large degree of disorder in chain packing.[21] For PLLA, it has also been reported recently that mesophase is formed under specific conditions of crystallization, such as melt-quenched PLLA-polyethylene glycol (PEG)-PLLA block copolymers,[22] uniaxial stretching around T_g,[23,24] and crystallization under high pressure CO_2 (α'' form).[25,26] The WAXD profiles of the samples prepared by above methods are identical, showing very broad peaks at around 11.7 and 22.4 nm^{-1}. It is concluded that a large degree of disorder is involved in the structure. Our results shown in Figure 1 are consistent with previously reported structures, suggesting that PLLA/SAE blend forms a thermodynamically quasi-stable mesophase, depending on the crystallization temperature. To the best of our knowledge, this is the first report of the mesophase formation for PLLA/plasticizer blend.

In order to gain more structural information of the mesophase, FTIR measurements were employed in this study. Figure 2 shows the FTIR spectra of PLLA/SAE blend crystallized at various temperatures. It has been reported that the three regions of the FTIR spectra are very sensitive for the structural changes

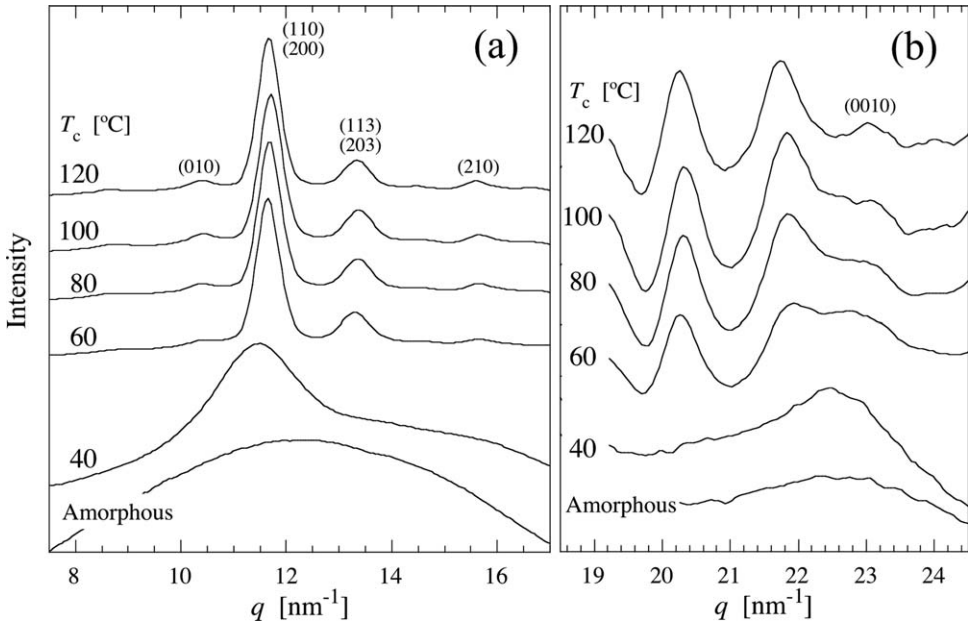

Figure 1. WAXD profiles of (a) lower q range and (b) higher q range of amorphous PLLA/SAE blends sample and PLLA/SAE crystallized at various crystallization temperatures from the melt.

that take place during the heat-treatment of semi-crystalline PLLA.[22] They are, the C–C backbone stretching region of 1000–800 cm^{-1} [Figure 2(a)], the region of 1500–1000 cm^{-1} where CH_3, CH bending, and C–O–C stretching vibration are related, and C=O stretching vibration region of 1810–1700 cm^{-1} [Figure 2(b)]. In Figure 2(a) of the C–C backbone stretching coupled with CH_3 rocking mode region,[27] the band at 923 cm^{-1}, which is assigned to be ordered-type 10/3 helical conformation of PLLA,[22,28] is clearly observed for the samples that crystallized above 60°C. The band is completely absent for amorphous PLLA, indicating no helical conformation in the quenched PLLA. It is interesting, however, that the band appears at lower wavenumber (916 cm^{-1}) when it is crystallized at 40°C. Since SAE has no particular band in this region, the band shift at around 920 cm^{-1} suggests the change in the conformational order and/or packing. The band shift was also reported by several researchers mentioned above.[22,23,26] It is concluded that the disordered-type 10/3 helical chains are roughly packed in mesophase of PLLA. In C=O stretching vibration region as shown in Figure 2(b), four characteristic bands, located at 1777 (shoulder), 1767 (shoulder), 1759, and 1749 cm^{-1}, are observed for T_c above 60°C. These bands are assigned as conformer bands of trans-trans (*tt*), gauche-trans (*gt*), gauche-gauche (*gg*), and trans-gauche (*tg*) respectively.[29–31] Among the conformers, *gt* is considered to be the most stable conformer to form 10/3 helix in the crystal. The *gt* band at 1759 cm^{-1} appeared for the samples crystallized above 60°C, indicating that 10/3 helical conformation has formed. The other conformational bands, especially that of 1749 cm^{-1}, become distinct at higher T_c although they are considered to be amorphous band. It was reported by Pan et al.[32] that the absorbances at 1777, 1767, and 1749 cm^{-1} were not clearly observed for α' form, while distinct for α form. They concluded that the band at 1777, 1767, and 1749 cm^{-1} could be assigned by the interaction of the carbonyl groups between adjacent chains in α crystal. Thus, it strongly suggests that the bands at 1749, 1767, and 1777 cm^{-1} are assigned both as conformational and the interaction band. In Figure 2(b), the sample crystallized at 40°C showed very broad band with its peak at 1753 cm^{-1}. It is attributed to the overlapping of several bands due to the smaller *gt* peak, i.e., its lower crystallinity.

The spectra of the samples crystallized at various T_c were analyzed as follows: (i) spectrum of amorphous PLLA was subtracted from the spectra in Figure 2(b) by adjusting the multiplying factor in order to remove all the conformational part of amorphous PLLA, which existed after crystallization and (ii) the subtracted spectra were fitted with four bands, which are crystalline conformational (*gt*) band (1759 cm^{-1}) and three interaction bands (1749, 1767, and 1777 cm^{-1}). Figure 3 shows the amorphous subtracted spectra of PLLA/SAE crystallized into α form [T_c = 120°C, (a)] and mesophase [T_c = 40°C, (b)]. The spectra, thus, indicate the absorbance of PLLA in the crystal. The curve-fittings with four bands were successfully carried out as shown with solid lines. The crystalline conformer band at 1759 cm^{-1} greatly differs in intensity between α form and mesophase, suggesting the difference in crystallinity as well as the perfectness of the crystal. Here, degrees of crystallinity (ϕ_c) and the interaction (ϕ_i) are estimated as follows:

$$\phi_c = \frac{A_c}{A_c + A_a + A_i} \quad (1)$$

$$\phi_i = \frac{A_i}{A_c + A_a + A_i} \quad (2)$$

A_c is the area of the band at 1759 cm^{-1} in Figure 3, which corresponds to *gt* conformer in the crystal, A_a is the area of conformers in amorphous state, A_i is the total area of three

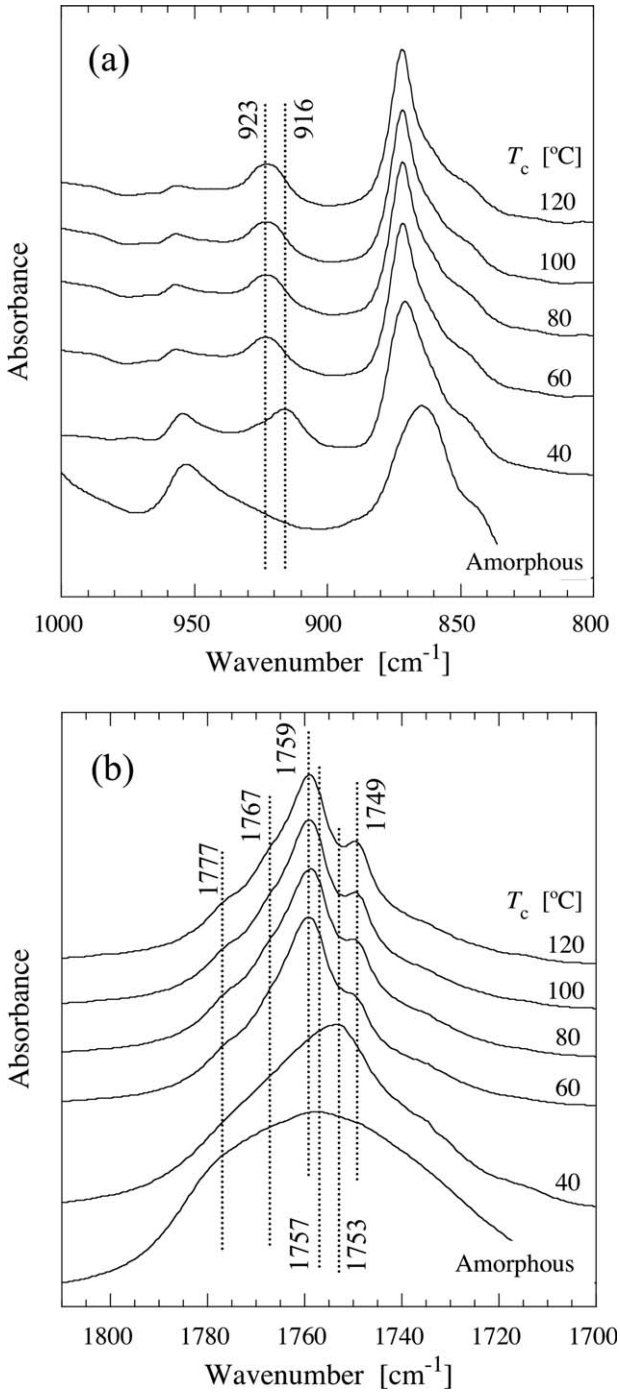

Figure 2. FTIR spectra of amorphous PLLA/SAE sample and PLLA/SAE blends crystallized at various crystallization temperatures from the melt in the frequency region of (a) 1000–800 cm^{-1} and (b) 1810–1700 cm^{-1}.

interaction bands (1749, 1767, and 1777 cm^{-1}) in the crystal. The ϕ_c as well as the ϕ_i were plotted against the T_c in Figure 4(a). The crystallinity of mesophase was estimated from eq. (1) to be 0.20. It was also estimated from WAXD profile as shown in Figure 1 to be 0.15, which showed a good agreement. It implies the validity of the method to estimate the crystallinity by means of FTIR measurement. It is clearly seen that the crystallinity increases with the increasing T_c up to 80°C while slight increase above 80°C. The degree of interaction shows the same trend as in the crystallinity. However, since the inter-chain interaction is also correlated with the crystallinity (i.e., increase in crystallinity leads to the increase in interaction), the degree of interaction was divided by the crystallinity in order to discuss the disordering in the packing of 10/3 helical chain. Figure 4(b) shows the plot of the relative degree of interaction (ϕ_i/ϕ_c) against T_c. For T_c above 80°C, it stays constant, indicating the same degree of packing order within a crystal. It is reasonable since only α form was crystallized in this temperature region as

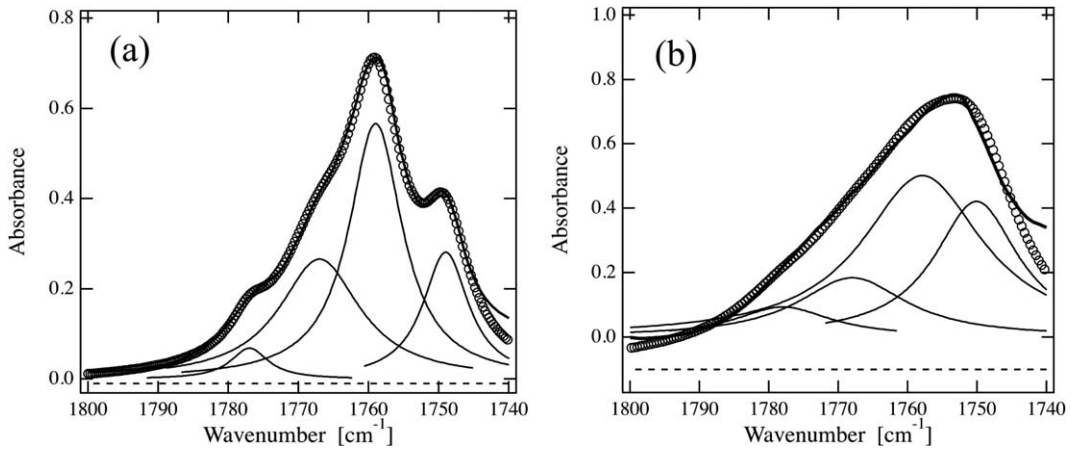

Figure 3. Carbonyl stretching region of PLLA/SAE blends at room temperature after isothermal crystallization at (a) 120°C and (b) 40°C. Experimental spectrum (open point), curve fitting components (thin line), baseline (dotted line), and fitting curve (thick line).

we demonstrated in Figure 1. For T_c at 60°C, the value is lower than that of α form. It is possibly due to the formation of α′ form or co-crystallization of α/α′ form during the isothermal crystallization at 60°C. When PLLA/SAE is crystallized at 40°C into mesophase, the relative degree of interaction shows much smaller value. It is a clear evidence that the mesophase has a larger amount of packing disorder, which reduces the interaction between adjacent chains. In α form of PLLA, 10/3 helical chains are aligned parallel and tightly packed in an orthorhombic unit cell. The interchain interaction of carbonyl group of PLLA chain is, thus, much stronger than that of amorphous or mesophase. The introduction of intra- and inter-chain disorder brings the reduction in interchain interaction as we have shown here and consequently the expansion in the spacing between the

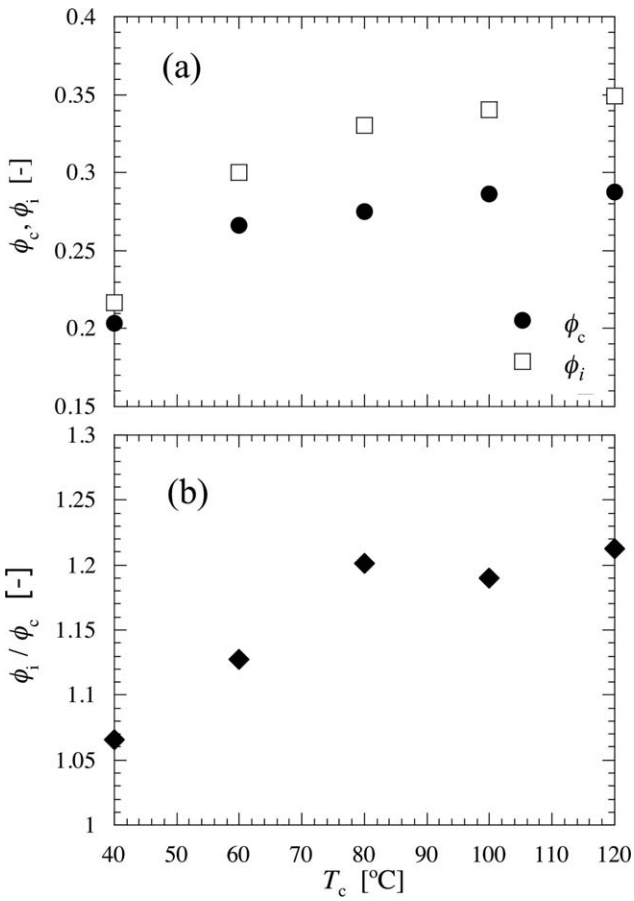

Figure 4. (a) Change of degrees of crystallinity and interaction at various crystallization temperatures. (b) Change of the value of relative degree of interaction at various crystallization temperatures.

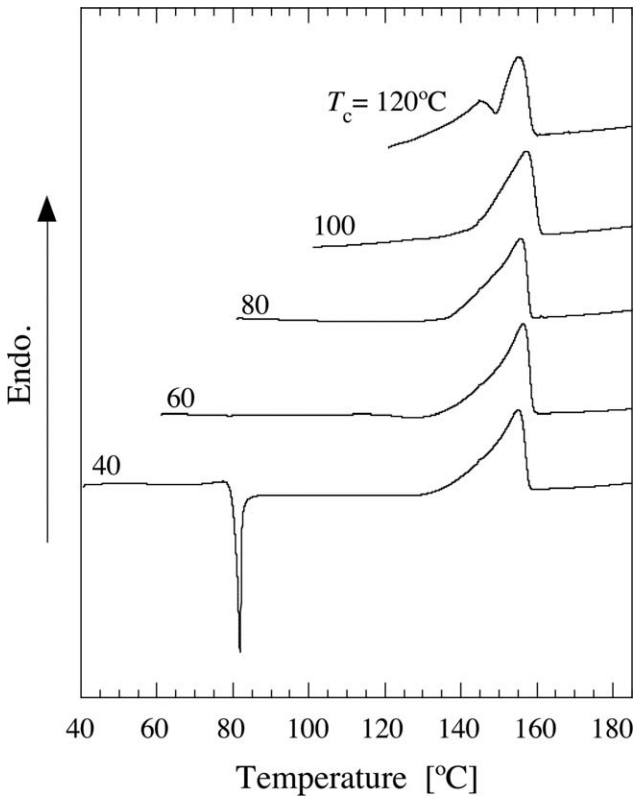

Figure 5. DSC heating curves of PLLA/SAE blends crystallized at various crystallization temperatures from the melt.

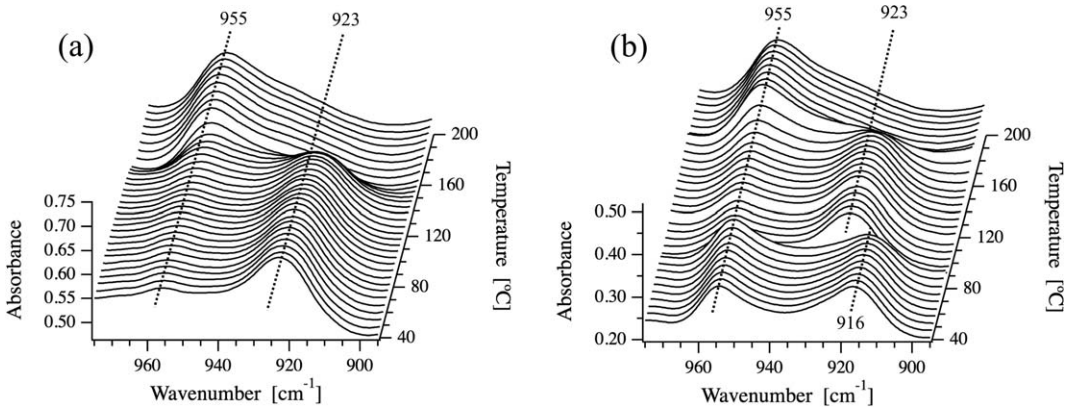

Figure 6. FTIR spectra evolution of PLLA/SAE blends crystallized at (a) 120°C and (b) 40°C during the heating process from 40 to 200°C in the backbone vibration region.

adjacent chains, which was shown as a low-q shift in WAXD profile in Figure 1.

We have reported the mesomorphic phase formation in PLLA/plasticizer blends. Among some findings of mesophase reported previously, the common feature of the condition, required for mesophase, seems to be the low temperature where its molecular motion is restricted. The restricted molecular mobility might lead to the mesophase with intermediate ordering between amorphous and crystal. Since the mesophase is thermodynamically quasi-stable, the structural change upon heating is expected as for iPP, which is to be discussed in the next section.

Thermal Behavior of Crystallized PLLA/SAE Blends

Figure 5 shows the DSC curves of the samples crystallized at various T_c during heating at the rate of 10°C/min. For T_c above 60°C, a broad endothermic peak, which comes from the melting of α crystal, appears at around 155°C. A small exothermic peak prior to the melting is observed only for T_c = 60°C. It was reported to be a transformation from disordered-type α′ form to ordered-type α form during heating.[8,19,22–24] Since some diffractions from α form were observed in this sample as shown in Figure 1, and the interaction was weaker as shown in Figure 4(b), it could be concluded that the co-crystallization of α′ and α form took place in PLLA/SAE crystallized at 60°C. For T_c above 80°C, no exothermic peak prior to the melting was observed. It indicates that PLLA crystallized into α form, which shows good agreement with WAXD and FTIR results as shown in Figures 1 and 4(b), respectively, whereas a peculiar exothermic peak appeared in the sample crystallized at 40°C. A very sharp peak at 80°C indicated that the crystallization took place during the heating. It should also be noted that the small endothermic peaks appears prior to the sharp exothermic peak at 80°C. As shown above, mesophase are formed when PLLA/SAE was crystallized at 40°C. The peculiar thermal behavior clearly indicates the phase transformation upon heating.

Figure 6 shows the changes in the FTIR spectra of PLLA/SAE, which were crystallized into α form [T_c = 120°C, (a)] and mesophase [T_c = 40°C, (b)], during heating at the rate of 1°C/min. It is already mentioned that the bands at 923 and 916 cm^{-1} are assigned to be 10/3 helical conformation of α/α′ form and mesophase, respectively. In the α form sample, the band at 923 cm^{-1} remains up to *ca.* 160°C, followed by a steep decrease due to the melting of α form crystal. While for the mesophase, characteristic change in the spectra was observed. The disordered-type 10/3 helix band at 916 cm^{-1} disappeared at 80°C and the α/α′ band appeared. The temperature coincides well with that of

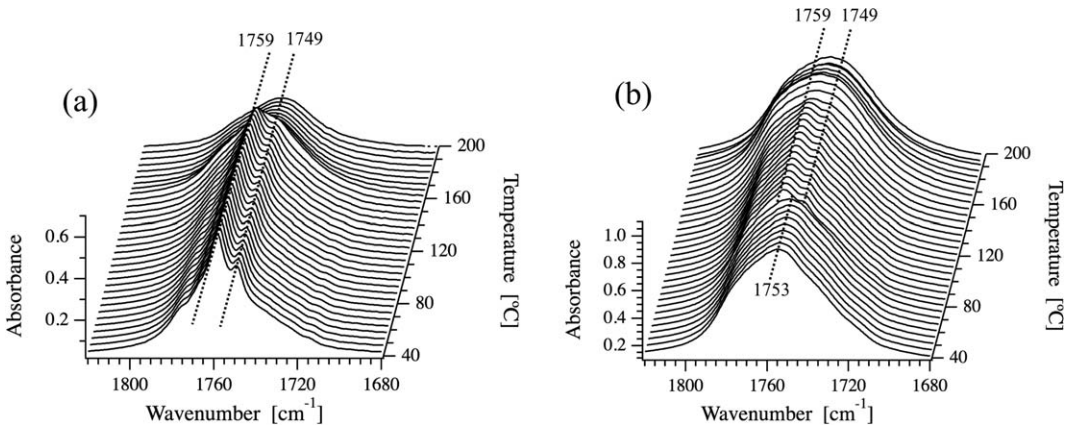

Figure 7. FTIR spectra evolution of PLLA/SAE blends crystallized at (a) 120°C and (b) 40°C during the heating process from 40 to 200°C in the Carbonyl stretching region.

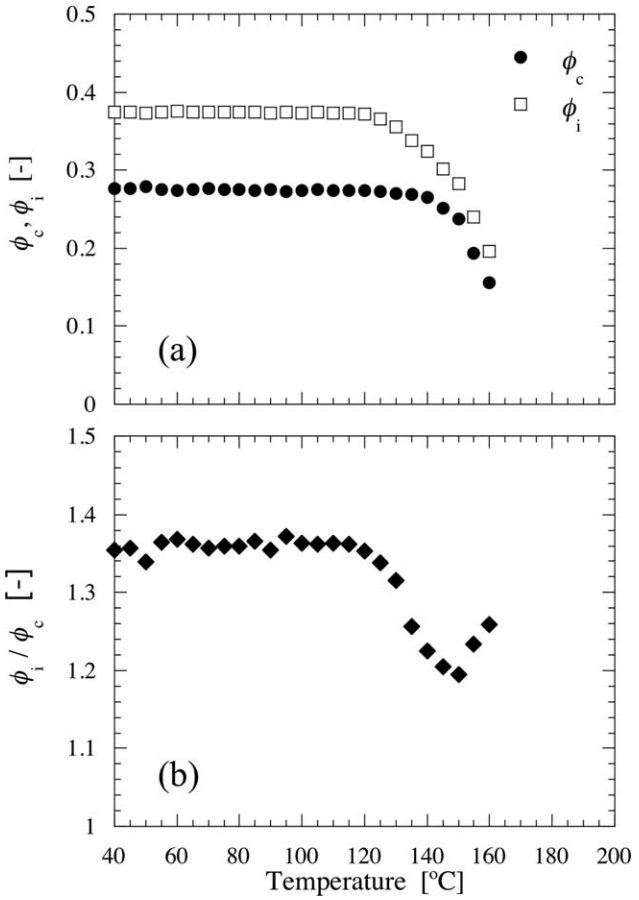

Figure 8. (a) Change of ϕ_c and ϕ_i for crystallized at 120°C during heating process. (b) Change of ϕ_i /ϕ_c for crystallized at 120°C during heating process.

DSC measurement as shown in Figure 5 which clearly indicates a phase transformation from mesophase to α or α′ form. The phase transformation is also observed in C=O vibration range as shown in Figure 7. α Form shows no change in the spectra up to the melting at *ca.* 160°C. In addition to the crystalline band at 1759 cm^{-1}, small band at 1749 cm^{-1}, which is assigned as an interaction band, remains unchanged before melting [Figure 7(a)]. For mesophase [Figure 7(b)], a very broad peak, which involves various conformers as well as the interactions, was seen below 80°C. While after the transformation at 80°C, the bands at 1759 and 1749 cm^{-1} appeared. It clearly indicates that the crystal formed after the phase transformation is α form, since α′ form is reported to show no distinct band at 1749 cm^{-1}. It is, thus, concluded that the mesophase transforms into α form via melting-recrystallization process.

The FTIR spectra shown in Figure 7 were subjected to the further analysis by the curve fitting method as described in the last section. Figure 8(a) shows the changes in the ϕ_c and the ϕ_i during the heating of α form (T_c = 120°C). The ϕ_c stays constant up to 140°C, followed by a steep decrease due to the melting of α form crystal. The ϕ_i also shows the same trend as of the ϕ_c, except that the decrease starts at lower temperature of 120°C. Accordingly, the relative degree of interaction plotted in Figure 8(b) shows slight decrease above 120°C. It suggests that the interaction between adjacent chains in the crystal gets weaker prior to the melting of α form crystal, while for the mesophase as shown in Figure 9, the ϕ_c and the ϕ_i show the decrease above 60°C, the steep increase at 80°C, the plateau above 90°C, followed by the decrease above 130°C due to the melting. The decrease above 60°C and the increase at 80°C clearly indicate that the phase transformation proceeds via melting–recrystallization process. It should also be noted that the ϕ_i after phase transformation of mesophase stays lower than that of α form shown in Figure 8(a), although the crystalline forms are equal. It may indicate that the interchain interaction differs between directly melt-crystallized α form and the mesophase-transfomed α form.

CONCLUSIONS

The effects of the crystallization temperature, T_c, on the crystal structure as well as its thermal behavior of plasticized poly(L-lactic acid) were investigated. The T_c dependence of the crystalline form of PLLA plasticized with 26 wt % of succinic acid-bis[2-[2-(2-methoxyethoxy)ethoxy]ethyl] ester (SAE) was different from that of PLLA homopolymer. The lower critical temperature for the formation of α form was 80°C, whereas 120°C for PLLA homopolymer. A peculiar disordered structure, namely mesophase, was observed when PLLA/SAE was

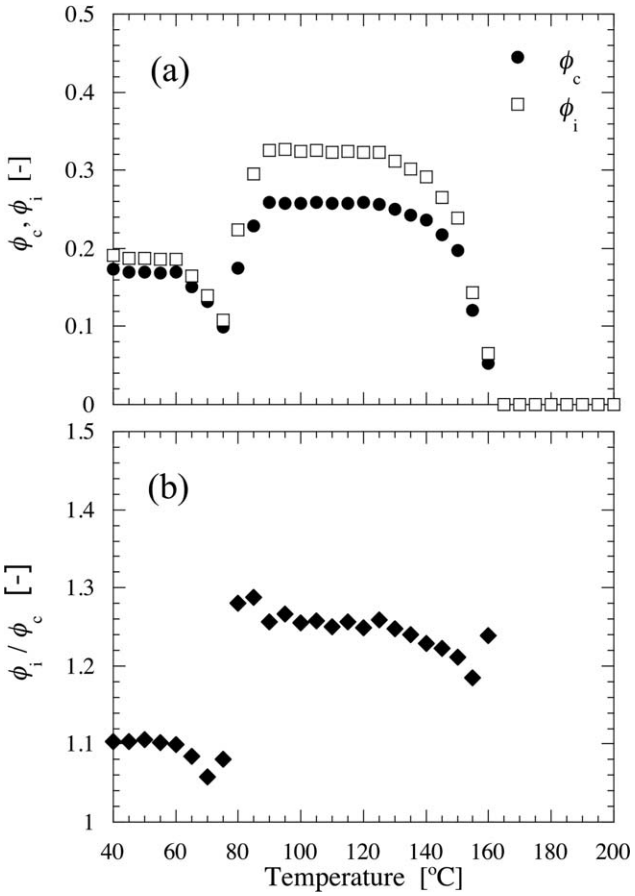

Figure 9. (a) Change of ϕ_c and ϕ_i for crystallized at 40°C during heating process. (b) Change of ϕ_i/ϕ_c for crystallized at 40°C during heating process.

crystallized at 40°C. The FTIR analysis, focusing on inter- and intra-chain interaction, indicated that the mesophase has a large amount of disorder both in 10/3 helical structure and in its packing manner.

Mesophase transformed into ordered-type α form upon heating. In addition to the increase in crystallinity at the transition temperature of 80°C, the inter-chain interaction also showed the increase due to the transformation into a form. Both crystallnity and interchain interaction in mesophase started to decrease at 60°C, which was well below the onset temperature of α formation. These findings lead to the conclusion that the mesophase-α transformation proceeds *via* melt recrystallization mechanism.

ACKNOWLEDGMENT

The synchrotron radiation experiments were performed at the BL40B2 of SPring-8 with the approval of the Japan Synchrotron Radiation Research Institute (JASRI) (Proposal No. 2010B1474, 2011A1336, and 2012A1348).

REFERENCES

1. Garlotta, D. *J. Polym. Environ.* **2001**, *9*, 63.
2. Pan, P.; Kai, W.; Zhu, B.; Dong, T.; Inoue, Y. *Macromolecules* **2007**, *40*, 6898.
3. Ke, T.; Sun, Xiuzhi. *J. Appl. Polym. Sci.* **2003**, *89*, 1203.
4. Li, H.; Huneault, M. A. *Polymer* **2007**, *48*, 6855.
5. Rahman, N.; Kawai, T.; Matsuba, G.; Nishida, K.; Kanaya, T.; Watanabe, H.; Okamoto, H.; Kato, M.; Usuki, A.; Matsuda, M.; Nakajima, K.; Honma, N. *Macromolecules*, **2009**, *42*, 4739.
6. Ljungberg, N.; Wesslén, B. *J. Appl. Polym. Sci.* **2002**, *86*, 1227.
7. Baiardo, M.; Frisoni, G.; Scandola, M.; Rimelen, M.; Lips, D.; Ruffieux, K.; Wintermantel, E. *J. Appl. Polym. Sci.* **2003**, *90*, 1731.
8. Kulinski, Z.; Piorkowska, E. *Polymer* **2005**, *46*, 10290.
9. Piorkowska, E.; Kulinski, Z.; Galeski, A.; Masirek, R. *Polymer* **2006**, *47*, 7178.
10. Koido, S.; Kawai, T.; Kuroda, S.; Nishida, K.; Kanaya, T.; Kato, M.; Kurose, T.; Nakajima, K. *Next Generation Polyolefins* **2011**, *5*, 107.
11. Cocca, M.; Di Lorenzo, ML.; Malinconico, M.; Frezza, V. *Eur. Polym. J.* **2011**, *47*, 1073.
12. Wasanasuk, K.; Tashiro, K. *Polymer,* **2011**, *52*, 6097.
13. Kawai, T.; Rahman, N.; Matsuba, G.; Nishida, K.; Kanaya, T.; Nakano, M.; Okamoto, H.; Kawada, J.; Usuki, A.; Honma, N.; Nakajima, K.; Matsuda, M. *Macromolecules* **2007**, *40*, 9463.
14. Zhang, J.; Tashiro, K.; Tsuji, H.; Domb, A. J. *Macromolecules* **2008**, *41*, 1352.
15. Qiu, J.; Wang, Z.; Yang, L.; Zhao, J.; Niu, Y.; Hsiao, B. S. *Polymer* **2007**, *48*, 6934.
16. Konishi, T.; Nishida, K.; Matsuba, G.; Kanaya, T. *Macromolecules* **2008**, *41*, 3157.
17. Minami, S.; Tsurutani, N.; Miyaji, H.; Fukao, K.; Miyamoto, Y. *Polymer* **2004**, *45*, 1413.
18. Konishi, T.; Nishida, K.; Kanaya, T.; Kaji, K. *Macromolecules* **2005**, *38*, 8749.
19. Nakaoki, T.; Ohira, Y.; Hayasi, H.; Horii, F. *Macromolecules* **1998**, *31*, 2705.
20. Ohira, Y.; Horii, F.; Nakaoki, T. *Macromolecules* **2000**, *33*, 5566.
21. Saraf, R. F. *Polymer* **1994**, *35*, 1359.
22. Zhang, J.; Duan, Y.; Abraham, J. D.; Ozaki, Y. *Macromolecules* **2010**, *43*, 4240.
23. Stoclet, G.; Seguela, R.; Lefebvre, J. M.; Rochas, C. *Macromolecules* **2010**, *43*, 7228.
24. Wasanasuk, K.; Tashiro, K. *Macromolecules* **2011**, *44*, 9650.
25. Marubayashi, H.; Akaishi, S.; Akasaka, S.; Asai, S.; Sumita, M. *Macromolecules* **2008**, *41*, 9192.
26. Marubayashi, H.; Asai, S.; Sumita, M. *Polymer* **2012**, *53*, 4262.
27. Kister, G.; Cassanas, G.; Vert, M. *Polymer* **1998**, *39*, 267.
28. Zhang, J.; Duan, Y.; Sato, H.; Tsuji, H.; Noda, I.; Yan, S.; Ozaki, Y. *Macromolecules* **2005**, *38*, 8012.
29. Meaurio, E.; Lopez-Rodriguez, N.; Sarasua, J. R. *Macromolecules* **2006**, *39*, 9291.
30. Meaurio, E.; Zuza, E.; Lopez-Rodriguez, N.; Sarasua, J. R. *J. Phys. Chem. B* **2006**, *110*, 5790.
31. Kang, S.; Hsu, S. L.; Shidham, H. D.; Smith, P. B.; Leugers, M. A.; Yang, X. *Macromolecules* **2001**, *34*, 4542.
32. Pan, P.; Zhu, B.; Kai, W.; Dong, T.; Inoue, Y. *Macromolecules* **2008**, *41*, 4296.